Translational Oncology 15 (2022) 101293

Contents lists available at ScienceDirect

Translational Oncology

journal homepage: www.elsevier.com/locate/tranon

Original Research

^{68}Ga-PSMA11 PET/CT for biochemically recurrent prostate cancer: Influence of dual-time and PMT- vs SiPM-based detectors

Heying Duan [a], Lucia Baratto [a], Negin Hatami [a], Tie Liang [a], Carina Mari Aparici [a], Guido Alejandro Davidzon [a], Andrei Iagaru [a,*]

[a] Department of Radiology, Division of Nuclear Medicine and Molecular Imaging, Stanford University, Stanford, CA, United States

ARTICLE INFO

Keywords:
Prostate cancer
^{68}Ga-PSMA11
PET/CT
SiPM
PMT

ABSTRACT

Objectives: ^{68}Ga-PSMA11 PET/CT is excellent for evaluating biochemically recurrent prostate cancer (BCR PC). Here, we compared the positivity rates of dual-time point imaging using a PET/CT scanner (DMI) with silicon photomultiplier (SiPM) detectors and a PET/CT scanner (D690) with photomultiplier tubes (PMT), in patients with BCR PC.

Methods: Fifty-eight patients were prospectively recruited and randomized to receive scans on DMI followed by D690 or vice-versa. Images from DMI were reconstructed using the block sequential regularized expectation maximization (BSREM) algorithm and images from D690 were reconstructed using ordered subset expectation maximization (OSEM), according to the vendor's recommendations. Two readers independently reviewed all images in randomized order, recorded the number and location of lesions, as well as standardized uptake value (SUV) measurements.

Results: Twenty-eight patients (group A) had DMI as first scanner followed by D690, while 30 patients (group B) underwent scans in reversed order. Mean PSA was 30±112.9 (range 0.3–600.66) ng/mL for group A and 41.5 ± 213.2 (range 0.21–1170) ng/mL for group B (P = 0.796). The positivity rate in group A was 78.6% (22/28 patients) vs. 73.3% (22/30 patients) in group B. Although the performance of the two scanners was equivalent on a per-patient basis, DMI identified 5 additional sites of suspected recurrent disease when used as first scanner. The second scan time point did not reveal additional abnormal uptake.

Conclusions: The delayed time point in ^{68}Ga-PSMA11 PET/CT did not show a higher positivity rate. SiPM-based PET/CT identified additional lesions. Further studies with larger cohorts are needed to confirm these results.

Introduction

Prostate cancer (PC) is the most diagnosed cancer and has the second highest mortality in the US [1]. Biochemical recurrence (BCR) is seen within 10 years in 20 – 40% of patients after initial treatment with radical prostatectomy (RP) and in 30 – 50% after radiation therapy (RT) [2]. A rising prostate specific antigen (PSA) level in patients with recurrent disease does not indicate the location of relapse. Differentiation of local, regional or systemic recurrence is of utmost importance for further disease management [3]. Despite development in anatomical imaging, there are still considerable limitations dependent on the size and site of relapse, especially in the early stage of BCR with low PSA values. For local disease detection, sensitivity ranges between 25% and 54% for transrectal ultrasound or contrast-enhanced computed tomography (CT) and is moderately improved by functional magnetic resonance imaging (MRI) techniques [3–6]. For detection of lymph node metastases, sensitivity ranges between 30% and 80% for CT or MRI [7].

Positron emission tomography/computed tomography (PET/CT) plays a significant role in the detection of recurrent PC by combining morphological and functional information, especially with radiotracers targeting the prostate-specific membrane antigen (PSMA). While ^{18}F-FDG has limited use in PC and may localize the site of disease in a small fraction of men with biochemical failure and negative conventional imaging [8], PSMA is overexpressed in more than 90% of cases [9]. Therefore, PSMA-targeting radiopharmaceuticals can be used from biopsy guidance to diagnose PC [10], to pre-surgical staging [11], to biochemical recurrence [12]. ^{68}Ga-PSMA11 binds to the extracellular domain of PSMA, followed by internalization into the cell and high accumulation in PC cells [13–15]. Despite the short half-life of ^{68}Ga, delayed imaging has been suggested in several studies for improved

* Corresponding author at: 300 Pasteur Drive, H2200, Stanford, CA 94305, United States.
E-mail address: aiagaru@stanford.edu (A. Iagaru).

https://doi.org/10.1016/j.tranon.2021.101293
Received 6 October 2021; Received in revised form 11 November 2021; Accepted 19 November 2021

lesion detection due to higher tumor to background contrast over time [16–18].

Technical improvements in PET/CT scanners enhance diagnostic accuracy with better image quality and higher spatial resolution. The Discovery MI (DMI) (GE Healthcare, Waukesha, WI, USA) is a PET/CT scanner with detectors that combine lutetium-based scintillator crystal arrays with a silicone photomultiplier (SiPM) bloc design. It allows for a new reconstruction method, the block sequential regularized expectation maximization (BSREM) (Q.Clear, GE Healthcare, Waukesha, WI, USA). The most commonly used reconstruction method for PET imaging is the ordered subset expectation maximization (OSEM) which uses 2 to 4 iterations since with every iteration, noise will increase thus decreasing image quality. BSREM is able to suppress the noise at higher iteration rates by introducing a noise penalty function, the β value, which controls the noise by voxel [19]. We previously showed the superiority of SiPM-based PET/CT against photomultiplier tubes (PMT)-based PET/CT (D690) in cancer patients undergoing ^{18}F-FDG imaging using OSEM as reconstruction method for both scanner systems. At the time of that study, the DMI PET/CT had not been approved by the Food and Drug Administration; therefore, the standard scanner was always used first, followed by SiPM-based PET/CT [20].

Here we evaluated the impact of SiPM- or PMT-based scanners used in randomized order, as well as dual-time point imaging, on positivity rates in BCR PC patients following a single injection of ^{68}Ga-PSMA11.

Material and methods

Participants

Patients with histo-pathologically proven prostate adenocarcinoma and rising PSA after initial definitive therapy with RP or RT were enrolled in this prospective study approved by the local institutional review board. BCR was diagnosed after prostatectomy with or without adjuvant radiotherapy at a PSA level of 0.2 ng/mL or greater, with a second confirmatory PSA level of at least 0.2 ng/mL [21]. For patients who had RT as initial treatment, BCR was diagnosed as rise of PSA of at least 2 ng/mL over the nadir [22]. Written informed consent was obtained from all included patients.

Participants were randomized to receive the first scan on either the DMI or D690 after a single injection of ^{68}Ga-PSMA11. The first PET/CT was performed 60 minutes after tracer injection according to guidelines [23], while the second scan was obtained immediately after the first scan. No specific patient preparation was required before the PET/CTs.

D690 PET/CT protocol

The CT scan was obtained for attenuation correction and anatomical localization using 120 kV, “smart” modulating mA and a 512×512 matrix size. Thereafter, a whole-body (vertex to mid-thighs) PET scan was acquired in 3D mode with time-of-flight (ToF) enabled. D690 has an axial field of view of 15.7 cm. Each field of view contains 47 slices (3.27 mm) and the overlap between bed positions was set to 11 slices (23%). PET data were corrected using the segmented attenuation data of the CT scan and reconstructed using the vendor-recommended reconstruction protocol with OSEM with 2 iterations and 24 subsets.

DMI PET/CT protocol

The CT scan was obtained for attenuation correction and anatomical localization using 120 kV, “smart” modulating mA and a 512×512 matrix size. Thereafter, a whole-body (vertex to mid-thighs) PET scan was acquired in 3D mode with ToF enabled. DMI has an axial field of view of 20 cm. Each field of view contains 71 slices (2.79 mm) and the overlap between bed positions was set to 17 slices (24%). PET data were corrected using the segmented attenuation data of the CT scan and reconstructed using the BSREM algorithm with a β value, the noise penalizing determining factor in BSREM, of 800 for its best performance [24].

When DMI or D690 were performed as second scan, a low-dose CT (10 mA) was obtained for attenuation correction and anatomic localization in order to minimize radiation exposure to participants.

Image analysis

Images were reviewed and analyzed independently in random order by two experienced readers (LB and HD, with 8 and 12 years of experience, respectively), using Advantage Workstation (GE Healthcare, Waukesha, WI, USA). Any focal uptake of ^{68}Ga-PSMA11 higher than the background and not associated with physiologic uptake was ruled as suspicious for malignancy [25]. Any disagreements were resolved by consensus read. Number and location of each detected lesion was recorded. Region-of-interests (ROI) of the same size were placed upon the area with the highest uptake for both studies to measure the maximum and mean standardized uptake value (SUV_{max} - SUV_{mean}) at a threshold of 42%. To determine the background activity, ROIs were placed on liver and gluteal fat, in areas of normal uptake. Impact on patient’s disease management was recorded from patient chart review.

Statistical analysis

Statistical analysis was performed with Stata v15.1 (Stata CorpLLC College Station, Texas). Continuous data are presented as mean ± standard deviation (SD), minimum (min) - maximum (max) values. A *P*-value of <0.05 was considered significant.

The participants were divided into two groups according to their scan sequence. Group A had imaging on the DMI first, followed by the D690. Group B was scanned on the D690 first, followed by the DMI. In order to normalize the SUVs measured from both scanners at different time points, the DMI and D690 had to be correlated to each other. We used an intraclass correlation which was calculated through a mixed effect model with clustering within patients based on the background organs liver and gluteal fat while taking the different acquisition time points into account. The same calculation method was applied when comparing lesion SUV_{max} and SUV_{mean} of DMI and D690 scaled to the background organs and time of scan.

Comparison of positivity rates between PSA levels was assessed by the Cochran-Mantel-Haenszel Test. For additional correlation with PSA, PSA doubling time and PSA velocity, an unpaired Wilcoxon rank-sum test was used. PSA doubling time and PSA velocity per month and year were obtained with the calculator provided by Memorial Sloan Kettering Cancer Center.

Results

Fifty-eight patients with BCR PC referred for ^{68}Ga-PSMA11 PET were prospectively enrolled in this study and randomized to be imaged on the DMI scanner first, followed by D690 or vice-versa.

The DMI-first followed by D690 patient group (group A, $n = 28$) had a mean age of 72.4 ± 6.6 (range 63 - 87) years vs. 69.6 ± 6.4 (range 59 - 90) years in the D690-first followed by DMI group (group B, $n = 30$). Initial definitive treatment was RP in 17/28 (60.7%) and RT in 11/28 patients (39.3%) in group A vs. 24/30 (80%) and 6/30 (20%) patients in group B.

Group A scans were acquired 57.7 ± 11.6 (range 44.5 - 82.8) minutes after injection of 146.5 ± 16.7 (range 111 – 200) MBq of ^{68}Ga-PSMA11 using DMI, followed by imaging on D690 at 83.4 ± 17 (range 66.8 - 139.8) minutes. The delay was 25.7 ± 7.7 (range 19 - 49.9) minutes. Group B scans were acquired 55.8 ± 8 (range 41.9 - 68.5) minutes post injection (pi) of 141 ± 16.3 (range 107.3 - 177.6) MBq ^{68}Ga-PSMA11 using D690 followed by DMI imaging at 86.8 ± 11.5 (range 72.3 - 114.9) minutes. The delay was 31 ± 8.6 (range 23 - 56.7) minutes.

Patients’ characteristics are shown in Table 1.

Table 1
Patient characteristics for both groups.

Parameter	Group A, $n = 28$ Value	Group B, $n = 30$ Value
Age (years)	72.4 ± 6.6 (range 63 - 87)	69.6 ± 6.4 (range 59 - 90)
Gleason Score	7.6 ± 0.9 (range 6 - 9)	7.4 ± 1 (range 6 - 9)
Initial Cancer Stage		
I	0%	6.7%
II	65.4%	36.6%
III	30.8%	36.6%
IV	3.8%	20%
Initial therapy		
RPE	17/28 patients (60.7%)	24/30 patients (80%)
RT	11/28 patients (39.3%)	6/30 patients (20%)
Median PSA (ng/mL)		
at the time of scan	30 ± 112.9 (range 0.3 – 600.66)	41.5 ± 213.2 ng/mL (range 0.21 - 1170)
PSA doubling time		
per month	9.8 ± 12.3	26.3 ± 97.9
per year	0.8 ± 1	2.2 ± 8.1
PSA velocity		
per month (ng/mL/month)	0.8 ± 1.5	8.1 ± 41.4
per year (ng/mL/year)	7.3 ± 12.9	97.8 ± 497.1
Mean ^{68}Ga-PSMA11 activity (MBq)	146.5 ± 16.7 (range 111 – 200)	141 ± 16.3 (range 107.3 - 177.6)
Time to acquisition of 1st scan (mins)	57.7 ± 11.6 (range 44.5 - 82.8)	55.8 ± 8 (range 41.9 - 68.5)
Time to acquisition of 2nd scan (mins)	83.4 ± 17 (range 66.8 - 139.8)	86.8 ± 11.5 (range 72.3 - 114.9)
Delay time between scans (mins)	25.7 ± 7.7 (range 19 - 49.9)	31 ± 8.6 (range 23 - 56.7)

PSA level and lesion detectability

Mean PSA level at the time of ^{68}Ga-PSMA11 PET/CT was 30 ± 112.9 (range 0.3 – 600.66) ng/mL vs. 41.5 ± 213.2 (range 0.21 - 1170) ng/mL, for groups A and B, respectively ($P = 0.796$). Both groups had a single outlier each (group A: 600.66 ng/mL and group B: 1170 ng/mL). In group A, 22/28 (78.6%) patients had a positive scan vs. 22/30 (73.3%) patients in group B.

As expected, the positivity rate increased with higher PSA levels. Patients with negative scans had a significantly lower PSA (mean PSA pos. vs. neg. scan: 6.2 ± 13.5 vs.1.6 ± 2.6, $P = 0.013$). For PSA <1.0 ng/mL, positivity rate was 57% for group A and 59% for group B. For PSA ≥1.0 ng/mL, positivity increased to 86% and 92%, respectively. The positivity rate per PSA level for the group A cohort was: 57% (PSA <1), 50% (1 ≤ PSA < 2), 100% (2 ≤ PSA < 5), and 85% (PSA ≥ 5), and for group B, 59% (PSA < 1), 100% (1 ≤ PSA < 2), 75% (2 ≤ PSA < 5), and 100% (PSA ≥ 5), respectively. The positivity rates were not significantly different between group A and group B within the different PSA levels ($P = 0.63$).

^{68}Ga-PSMA11 PET positivity rate per PSA doubling time was 60%, 89%, 40% and 100% and 100%, 60% 63% and 80% for group A and group B, respectively, for doubling time of 0–3 month, 3–6 months, 6–12 months and >12 months.

Patients with positive scans had significantly higher PSA velocity per month ($P = 0.001$) and per year ($P = 0.001$), but not significantly higher doubling time per month ($P = 0.288$), nor per year ($P = 0.358$). These findings are summarized in Table 2.

The overall sensitivity, specificity, positive predictive value (PPV) and negative predictive value (NPV) with 95% confidence interval (CI) were similar for both scanners, as indicated in Table 3. Sensitivity, specificity, PPV and NPV of DMI and D690 were additionally stratified to PSA groups of 0.2 to < 0.5, 0.5 to < 1.0, 1.0 to < 2.0, 2.0 to < 5.0, and ≥ 5.0. DMI was superior in the low PSA group while D690 showed higher specificity and PPV in the PSA 2.0 to < 5.0 group. All data are shown in Supplemental Table S1.

Table 2
Positivity rates of ^{68}Ga-PSMA11 PET/CT groups A and B, based on PSA level (ng/mL), PSA doubling time (months) and PSA velocity/month (ng/mL).

Group A	Positive PET (*n*)	Negative PET (*n*)	Percentage positive scan
PSA < 1	4	3	57%
1 ≤ PSA < 2	1	1	50%
2 ≤ PSA < 5	6	0	100%
PSA ≥ 5	11	2	85%
Total	22	6	79%
PSA Doubling time (months)			
0 - 3	3	2	60%
3 - 6	8	1	89%
6 - 12	2	3	40%
> 12	5	0	100%
PSA velocity/month (ng/mL)			
0 – 0.5	12	5	74%
0.5 - 1	2	0	100%
1 - 5	3	0	100%
> 5	2	0	100%
Group B	Positive PET (*n*)	Negative PET (*n*)	Percentage positive scan
PSA < 1	10	7	59%
1 ≤ PSA < 2	3	0	100%
2 ≤ PSA < 5	3	1	75%
PSA ≥ 5	6	0	100%
Total	22	8	73%
PSA Doubling time (months)			
0 - 3	8	0	100%
3 - 6	3	2	60%
6 - 12	5	3	63%
> 12	4	1	80%
PSA velocity/month (ng/mL)			
0 – 0.5	17	7	71%
0.5 - 1	1	0	100%
1 - 5	2	0	100%
> 5	1	0	100%

Table 3
The overall sensitivity, specificity, positive predictive value (PPV) and negative predictive value (NPV) with 95% confidence interval (CI) for DMI and D690.

	Sensitivity	Specificity	Positive predictive value	Negative predictive value
DMI	100% (93.7, 100)	83.5% (74.6, 90.3)	78.1% (66.9, 86.9)	100% (95.5, 100)
D690	100% (89.7, 100)	88.1% (80.9, 93.4)	70.8% (55.9, 83)	100% (96.5, 100)

Sites of disease detection

The inter-scanner correlation based on the background organs showed that both scanners were positively correlated, more for liver (ICC 0.764, 95% CI 0.590 - 0.879) than gluteal fat (ICC 0.183, 95% CI 0.031 - 0.609) (Table 4a).

In group A, 77 lesions were detected: 12 in the prostate bed; 17 in pelvic, 12 in paraaortic, and 9 in mediastinal lymph nodes; 25 osseous and 2 lung lesions. Five sites of suspected recurrent disease were only seen on DMI PET/CT when performed as first scan: 2 bilateral prostate bed lesions and 1 left internal iliac lymph node in one patient; 1 lung lesion in a second patient (Fig. 2); 1 pelvic lymph node in a third patient.

In group B, 49 lesions were recorded. All were identified on both PET/CT systems: 10 in the prostate bed; 15 in pelvic, 10 in paraaortic, 6 in mediastinal lymph nodes, and 8 in the skeleton.

No additional findings were seen in the delayed images, neither on DMI nor D690.

Table 4
Inter-scanner agreement analysis.

a) DMI vs. D690 based on SUV_{max} and SUV_{mean} of the background organs, liver and gluteal fat, are positively correlated

	SUV_{max}		SUV_{mean}	
Location	**ICC**	**95% CI**	**ICC**	**95% CI**
Liver	0.764	0.590–0.879	0.814	0.655–0.910
Gluteal fat	0.183	0.031–0.609	0.088	0.037–0.196

b) Comparison of lesions SUV_{max} and SUV_{mean} of both scanners, scaled to background organs, liver and gluteal fat, and corrected for the time of scan.

	SUV_{max}			SUV_{mean}		
Liver	**coef**	***P***	**95% CI**	**coef**	***P***	**95% CI**
Lesion SUV	0.765	0.098	0.556–1.051	1.016	0.582	0.961–1.074
Gluteal fat	**coef**	***P***	**95% CI**	**coef**	***P***	**95% CI**
Lesion SUV	0.828	0.275	0.590–1.162	0.846	0.059	0.712–1.007

ICC = Intraclass Correlation.
Coef = Coefficient.
CI = Confidence interval.

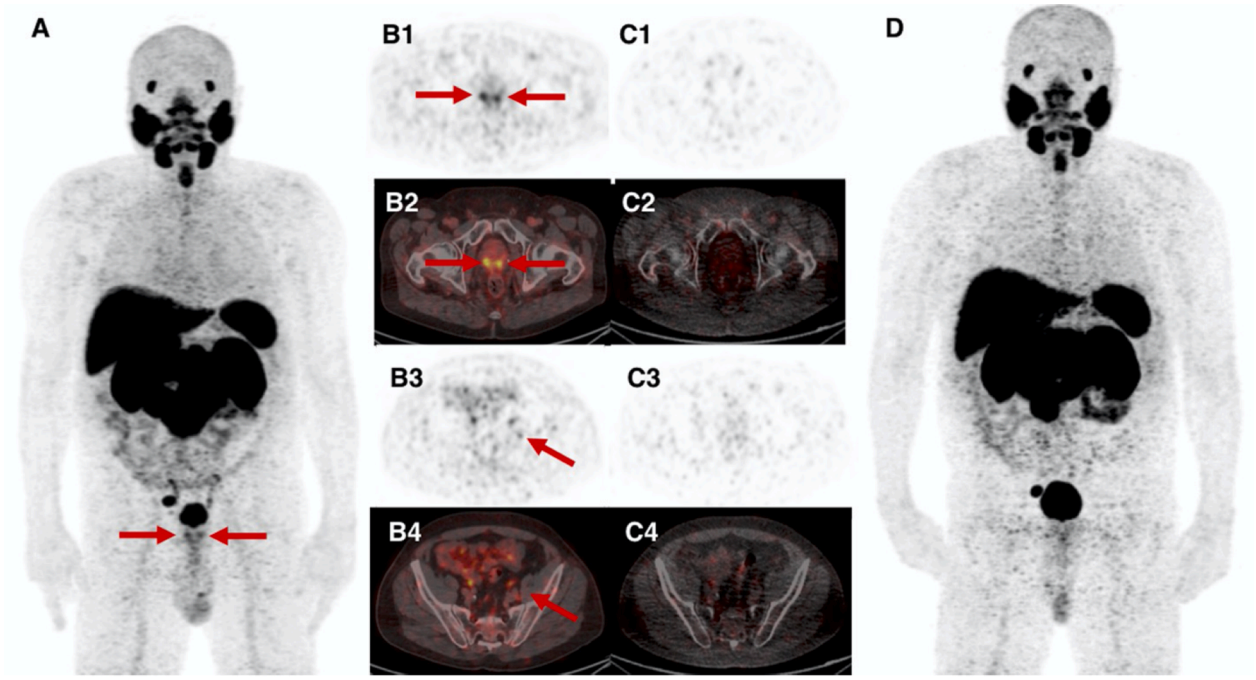

Fig. 1. 68-year-old patient with BCR PC (PSA 6.2 ng/mL) after initial radiation therapy. ^{68}Ga-PSMA11 DMI images (A, maximum intensity projection - MIP; B1-B4, axial PET and fused PET/CT images) show focal uptake bilateral in the prostate bed and a sub-centimeter left internal iliac lymph node (arrows), which are not seen on images from D690 scanner (C1–4, axial PET and fused PET/CT images; D, MIP). Prostate biopsy revealed prostate adenocarcinoma in the medial base, medial apex and lateral mid, only on the right side and benign tissue in the left prostate, with radiation effect. Subsequently, androgen deprivation therapy and proton beam therapy to the right pelvic and right iliac nodes as the disease burden was located on the right side. Therefore, we have no correlation for whether the left internal iliac lymph node might be false positive. PSA decreased to undetectable level within 6 months after ^{68}Ga-PSMA11 imaging.

In group A, mean SUV_{max} was 12.4 ± 11.7 (range 1.6 - 63.9) for DMI vs. 8.9 ± 8.9 (range 1.4 - 40.1) for D690. In group B, SUV_{max} from DMI was 18.7 ± 14.6 (range 3.7 - 70.3) vs. D690 11.2 ± 10.4 (range 3.3 - 47.2). For statistical analysis, SUV_{max} values were corrected for the time of scan and scaled to the respective scanner and background organs and showed no statistically significant difference (scaled to liver: $P = 0.098$; scaled to gluteal fat $P = 0.275$). Data is shown in Table 4b. When comparing the uncorrected mean SUV_{max} and SUV_{mean}, lesion SUV_{max} from the DMI were significantly higher than from the D690 regardless of whether performed as first ($P = 0.029$) or second scan ($P = 0.003$). SUV_{mean} was not significantly different for both PET/CT systems (group A: 0.694, group B: 0.599). All uncorrected SUV data are shown in Table 5.

Discussion

The role of PET/CT in oncology is indispensable. Recent technical developments in hybrid PET/CT have resulted in better image quality, thus leading to optimized treatment options. The National Electrical Manufacturers Association (NEMA) has characterized sensitivity, spatial resolution, scatter fraction, noise-equivalent counting rate, counting rate accuracy and image quality in its NEMA NU2 2012 standards. The DMI PET/CT scanner has high sensitivity due to its lutetium-based scintillator crystal arrays combined with a SiPM bloc design [26]. In this prospective study of ^{68}Ga-PSMA11 PET imaging of BCR PC, we evaluated the positivity rate of the PET/CT scanner using SiPM detectors compared to a standard of care PMT-based PET. Alberts et al. reported on ^{68}Ga-PSMA11 PET using digital vs. analog PET from a different vendor [27] but used matched patient cohorts. In this study, the same patients underwent scanning with both type of scanners. Due to the different scanners and the different acquisition time points, we had to normalize the obtained lesion SUV_{max} and SUV_{mean} to the background organs, scanners and correct for the time of scan. When mean SUV_{max} values from the DMI and D690 systems were compared, they were

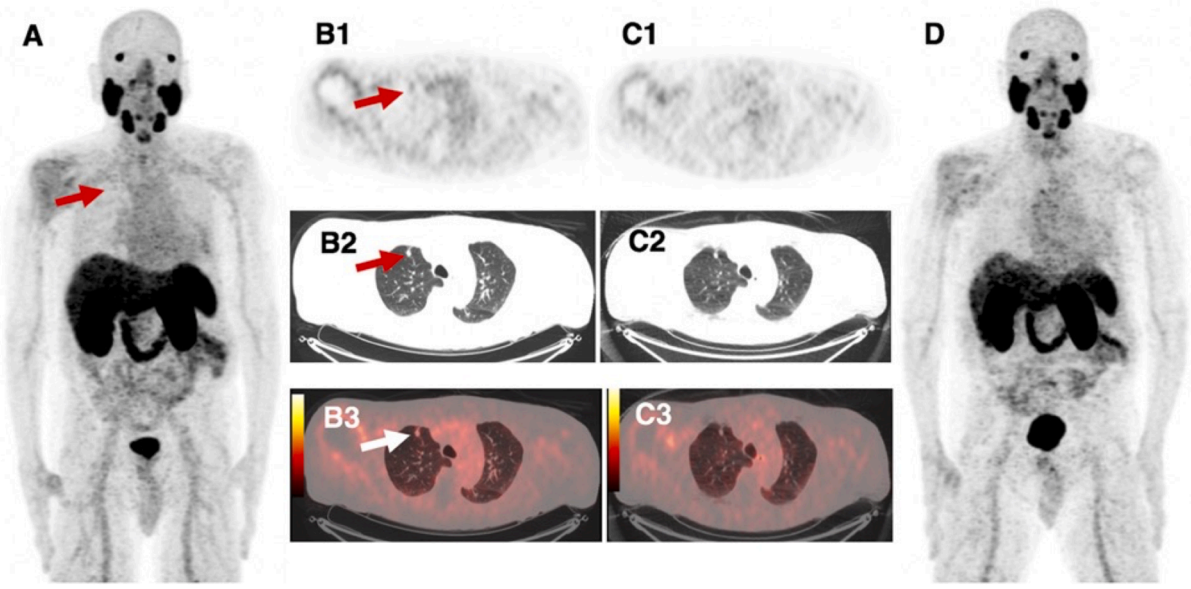

Fig. 2. 87-year-old patient with BCR PC (PSA 0.9 ng/mL) after initial radiation therapy. ^{68}Ga-PSMA11 DMI images (A, MIP; B1-B3, axial PET, CT and fused PET/CT images, respectively) show focal uptake in a 10 mm lung nodule (arrow), not seen in the D690 scan (C1-C3, axial PET, CT and fused PET/CT images, respectively; D, MIP). This lesion has been previously diagnosed by ^{68}Ga-PSMA11 PET/CT and ADT was initiated 4 months prior to recent ^{68}Ga-PSMA11 imaging which showed a decrease in size as response to treatment as well as a decrease in PSA. We therefore ruled the lung nodule as PC metastasis.

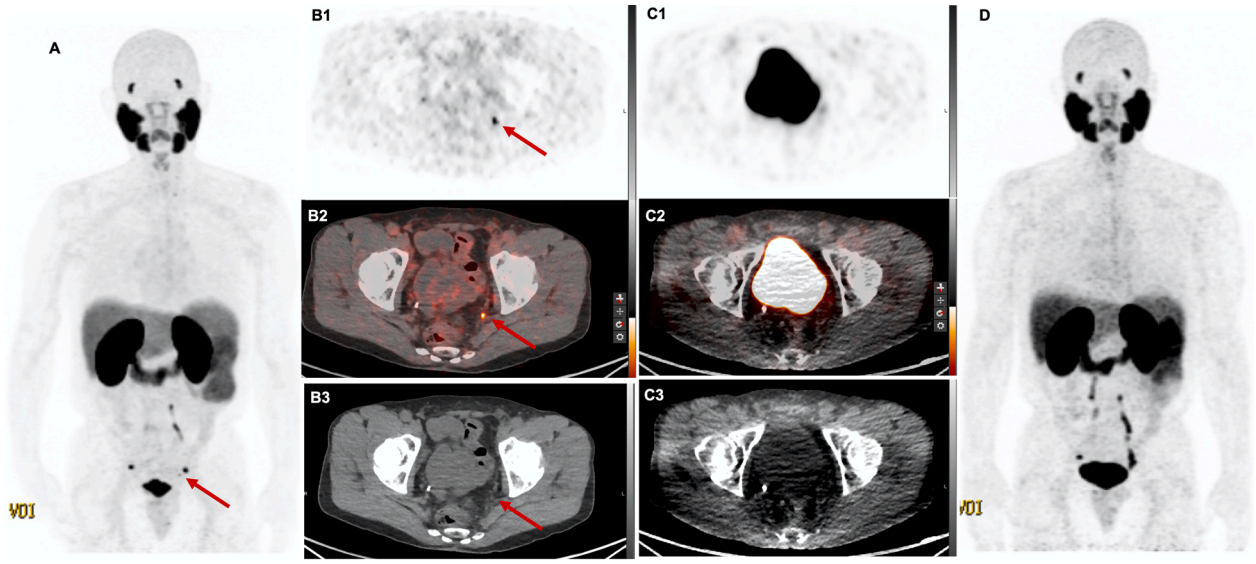

Fig. 3. 69-year-old patient with BCR PC (PSA 4.2 ng/mL) after initial radical prostatectomy. ^{68}Ga-PSMA11 DMI images (A, MIP; B1-B3, axial PET, fused PET/CT images and CT, respectively) show focal uptake in a 4 × 3 mm left pelvic lymph node (arrow), which was missed in images from D690 scanner (C1–3, axial PET, fused PET/CT images and CT, respectively; D, MIP). This lesion was also seen in a previous research ^{68}Ga-RM2 PET/MRI. Disease management did not change as the patient refused recommended RT.

statistically not significant on a per-patient analysis. Uncorrected, SUV_{max} of the DMI was generally higher whether used as first or second scanner. Even when D690 was performed as second scan with delayed increased uptake attributing to higher SUVs, mean SUV_{max} in the SiPM PET/CT group was still higher. This is consistent with previously published data reporting on significantly higher SUV for patients scanned with ^{18}F-FDG on a digital PET/CT as compared to an analog scanner [28, 29]. We believe that the consistently higher mean SUV_{max} values from the DMI resulted from the detector technology as the conversion of photons into a digital signal leads to higher sensitivity, expressed by higher SUV_{max} [20,28-31].

The overall sensitivity, specificity, PPV and NPV were similar for both scanners. However, in PSA sub-analyses, DMI was superior at low PSA values while D690 showed higher specificity and PPV at higher PSA. As ^{68}Ga-PSMA11 PET imaging is limited at very low PSA values, imaging with the new generation digital PET/CT scanner might give more certainty in diagnosing PC lesions at BCR. In a recently published retrospective analysis, Alberts et al. showed similar results, again in a matched pair cohort of patients undergoing digital or analog PET/CT in PC patients after RP or RP combined with RT [32].

As expected, higher PSA values showed higher detectability rates. The positivity rate was lower for low PSA values: 57% and 59% for PSA <1 ng/ml, increased for PSA >1 ng/ml to 86% and 92% in groups A and B, respectively. These findings are consistent with previous studies

Table 5
Comparison of SUV_{max} of detected lesions and background organs, significance shown are not scaled to background organs and uncorrected for the time of scan.

a) Group A: DMI performed first, followed by the D690						
	SUV_{max}			SUV_{mean}		
	Lesions	Liver	Gluteal fat	Lesions	Liver	Gluteal fat
DMI	12.4 ± 11.7	6.09 ± 3.5	0.41 ± 0.2	4.63 ± 5.87	4.88 ± 2.62	0.21 ± 0.09
D690	8.9 ± 8.9	5.51 ± 2.29	0.41 ± 0.18	4.28 ± 5.05	4.39 ± 1.98	0.32 ± 0.53
P	0.029*	0.467	0.889	0.694	0.434	0.273
b) Group B: D690 performed first, followed by the DMI						
	SUV_{max}			SUV_{mean}		
	Lesions	Liver	Gluteal fat	Lesions	Liver	Gluteal fat
D690	10.44 ± 10.08	6.69 ± 1.7	0.36 ± 0.15	4.8 ± 5.47	5.3 ± 1.43	0.21 ± 0.09
DMI	18.05 ± 14.28	6.58 ± 2.05	0.4 ± 0.14	5.43 ± 6.34	5.07 ± 1.63	0.19 ± 0.05
P	0.003*	0.822	0.333	0.599	0.560	0.177

[33–35]. A higher PSA velocity was also positively correlated to a higher positivity rate, but not PSA doubling time. Previous studies have shown that PSA velocity is a more useful predictor for PC aggressiveness [36, 37]. D'Amico et al. demonstrated that a PSA velocity of >2 ng/mL/y is associated with a decreased time to PC-specific and all-cause mortality as opposed to 2.0 ng/mL/y or less [38]. Our results on PSA velocity are consistent with our previous findings evaluating ^{68}Ga-RM2 PET/MRI in BCR PC with negative conventional imaging [39]. If further, larger studies confirm these results, PSA velocity might be a good tool in prediction of scan positivity. Additionally, an elevated PSA with low PSA velocity and negative ^{68}Ga-PSMA11 imaging might carry a benign prognosis as opposed to an elevated PSA with high PSA velocity and positive PET/CT findings.

In imaging with PSMA tracers, multiple authors [16,40,41] reported that delayed imaging is beneficial in primary and BCR PC especially in the interpretation of equivocal findings as it improves the tumor-to-nontumor ratio. However, Schmuck et al. [41] found in ^{68}Ga-PSMA I&T that despite the higher contrast in delayed imaging, it did not lead to overall higher detection rates. Afshar-Oromieh et al. [16] showed high detection rate of PC lesions 1 h after ^{68}Ga-PSMA11 injection, but delayed imaging at 3 h pi revealed additional findings. Other authors reported that early imaging at 5 min pi [42] and 20 min pi [43] lead to as favorable detection rates as standard imaging at 1 h pi. In our study, additional findings were exclusively seen on the DMI when used as first scanner. Delayed imaging did not result in identification of additional lesions.

We followed up patients up to 24 months using chart review. Histopathological correlation was only available in a minority of patients (10/58). Therefore, a limitation of this study is that we report positivity rates, not detection rates. However, published guidelines indicate that uptake above background should be considered positive for disease until proven otherwise given the high sensitivity and accuracy of ^{68}Ga-PSMA11 [44]. Another limitation is that the DMI images were reconstructed with BSREM while images from the D690 were reconstructed with OSEM. We previously showed the superiority of DMI versus D690 in imaging with ^{18}F -FDG where images from both scanners were reconstructed using OSEM.

Conclusion

Both standard PMT- and the new generation SiPM-based PET/CT systems showed high positivity rates using ^{68}Ga-PSMA11 in BCR PC. However, SiPM-based DMI identified a small number of additional lesions compared to PMT-based D690 and showed higher sensitivity, specificity at low PSA range. Delayed imaging did not contribute to higher positivity rates in our cohort.

Declaration of Competing Interest

The study was partially supported by GE Healthcare. The authors declare no conflict of interest.

Funding

The study was partially supported by GE Healthcare.

Authors statement

Heying Duan: data analyses, manuscript writing and editing
Lucia Baratto: data analyses, manuscript writing and editing
Negin Hatami: data collection
Tie Liang: statistical analyses
Carina Mari Aparici: manuscript editing
Guido Davidzon: manuscript editing
Andrei Iagaru: content planning, data analyses, manuscript editing

References

[1] R.L. Siegel, K.D. Miller, H.E. Fuchs, A. Jemal, Cancer Statistics, 2021, CA Cancer J. Clin. 71 (1) (2021) 7–33.
[2] H. Isbarn, M. Wanner, G. Salomon, T. Steuber, T. Schlomm, J. Kollermann, Long-term data on the survival of patients with prostate cancer treated with radical prostatectomy in the prostate-specific antigen era, BJU Int. 106 (1) (2010) 37–43.
[3] S.R. Bott, Management of recurrent disease after radical prostatectomy, Prostate Cancer Prostatic Dis. 7 (3) (2004) 211–216.
[4] V. Panebianco, A. Sciarra, D. Lisi, F. Galati, V. Buonocore, C. Catalano, Prostate cancer: 1HMRS-DCEMR at 3T versus [(18)F]choline PET/CT in the detection of local prostate cancer recurrence in men with biochemical progression after radical retropubic prostatectomy (RRP), Eur. J. Radiol. 81 (4) (2012) 700–708.
[5] A.J. Beer, M. Eiber, M. Souvatzoglou, M. Schwaiger, B.J. Krause, Radionuclide and hybrid imaging of recurrent prostate cancer, Lancet Oncol. 12 (2) (2011) 181–191.
[6] D.A. Woodrum, A. Kawashima, K.R. Gorny, L.A. Mynderse, Prostate cancer: state of the art imaging and focal treatment, Clin. Radiol. 72 (8) (2017) 665–679.
[7] R.H. Oyen, H.P. Van Poppel, F.E. Ameye, W.A. Van de Voorde, A.L. Baert, L. V. Baert, Lymph node staging of localized prostatic carcinoma with CT and CT-guided fine-needle aspiration biopsy: prospective study of 285 patients, Radiology 190 (2) (1994) 315–322.
[8] H. Jadvar, Is there use for FDG-PET in prostate cancer? Semin. Nucl. Med. 46 (6) (2016) 502–506.
[9] S.D. Sweat, A. Pacelli, G.P. Murphy, D.G. Bostwick, Prostate-specific membrane antigen expression is greatest in prostate adenocarcinoma and lymph node metastases, UrologyUrology 52 (4) (1998) 637–640.
[10] D.A. Ferraro, A.S. Becker, B. Kranzbühler, I. Mebert, A. Baltensperger, K. G. Zeimpekis, Diagnostic performance of (68)Ga-PSMA-11 PET/MRI-guided biopsy in patients with suspected prostate cancer: a prospective single-center study, Eur. J. Nucl. Med. Mol. Imaging 48 (10) (2021) 3315–3324.
[11] S.Y. Park, C. Zacharias, C. Harrison, R.E. Fan, C. Kunder, N. Hatami, Gallium 68 PSMA-11 PET/MR imaging in patients with intermediate- or high-risk prostate cancer, RadiologyRadiology 288 (2) (2018) 495–505.
[12] H. Song, C. Harrison, H. Duan, K. Guja, N. Hatami, B.L. Franc, Prospective evaluation of (18)F-DCFPyL PET/CT in biochemically recurrent prostate cancer in an academic center: a focus on disease localization and changes in management, J. Nucl. Med. 61 (4) (2020) 546–551.
[13] A. Afshar-Oromieh, A. Malcher, M. Eder, M. Eisenhut, H.G. Linhart, B. A. Hadaschik, PET imaging with a [68Ga]gallium-labelled PSMA ligand for the diagnosis of prostate cancer: biodistribution in humans and first evaluation of tumour lesions, Eur. J. Nucl. Med. Mol. Imaging 40 (4) (2013) 486–495.
[14] M. Eder, M. Schafer, U. Bauder-Wust, W.E. Hull, C. Wangler, W. Mier, 68Ga-complex lipophilicity and the targeting property of a urea-based PSMA inhibitor for PET imaging, Bioconjug. Chem. 23 (4) (2012) 688–697.
[15] T. Maurer, M. Eiber, M. Schwaiger, J.E. Gschwend, Current use of PSMA-PET in prostate cancer management, Nat Rev Urol 13 (4) (2016) 226–235.
[16] A. Afshar-Oromieh, L.P. Sattler, W. Mier, B.A. Hadaschik, J. Debus, T. Holland-Letz, The Clinical Impact of Additional Late PET/CT Imaging with (68)Ga-PSMA-11 (HBED-CC) in the Diagnosis of Prostate Cancer, J. Nucl. Med. 58 (5) (2017) 750–755.
[17] T. Derlin, D. Weiberg, C. von Klot, H.J. Wester, C. Henkenberens, T.L. Ross, (68)Ga-PSMA I&T PET/CT for assessment of prostate cancer: evaluation of image quality after forced diuresis and delayed imaging, Eur. Radiol. 26 (12) (2016) 4345–4353.
[18] C. Can, H. Komek, Contribution of 5th minute and 2nd hour images to standard imaging in ((68)Ga)PSMA 11 PET/CT, Ann. Nucl. Med. 34 (3) (2020) 163–173.
[19] L. Baratto, H. Duan, V. Ferri, M. Khalighi, A. Iagaru, The effect of various beta values on image quality and semiquantitative measurements in 68Ga-RM2 and

68Ga-PSMA-11 PET/MRI images reconstructed with a block sequential regularized expectation maximization algorithm, Clin. Nucl. Med. 45 (7) (2020) 506–513.
[20] L. Baratto, S.Y. Park, N. Hatami, G. Davidzon, S. Srinivas, S.S. Gambhir, 18F-FDG silicon photomultiplier PET/CT: a pilot study comparing semi-quantitative measurements with standard PET/CT, PLoS ONE 12 (6) (2017), e0178936.
[21] M.S. Cookson, G. Aus, A.L. Burnett, E.D. Canby-Hagino, A.V. D'Amico, R. R. Dmochowski, Variation in the definition of biochemical recurrence in patients treated for localized prostate cancer: the American urological association prostate guidelines for localized prostate cancer update panel report and recommendations for a standard in the reporting of surgical outcomes, J. Urol. 177 (2) (2007) 540–545.
[22] M. Roach III, G. Hanks, H. Thames Jr, P. Schellhammer, W.U. Shipley, G.H. Sokol, Defining biochemical failure following radiotherapy with or without hormonal therapy in men with clinically localized prostate cancer: recommendations of the RTOG-ASTRO Phoenix Consensus Conference, International Journal of Radiation Oncology* Biology* Physics 65 (4) (2006) 965–974.
[23] W.P. Fendler, M. Eiber, M. Beheshti, J. Bomanji, F. Ceci, S. Cho, (68)Ga-PSMA PET/CT: joint EANM and SNMMI procedure guideline for prostate cancer imaging: version 1.0, Eur. J. Nucl. Med. Mol. Imaging 44 (6) (2017) 1014–1024.
[24] J. Lantos, E.S. Mittra, C.S. Levin, A. Iagaru, Standard OSEM vs. regularized PET image reconstruction: qualitative and quantitative comparison using phantom data and various clinical radiopharmaceuticals, Am J Nucl Med Mol Imaging 8 (2) (2018) 110–118.
[25] I. Rauscher, T. Maurer, W.P. Fendler, W.H. Sommer, M. Schwaiger, M. Eiber, (68) Ga-PSMA ligand PET/CT in patients with prostate cancer: how we review and report, Cancer Imaging 16 (1) (2016) 14.
[26] D.F.C. Hsu, E. Ilan, W.T. Peterson, J. Uribe, M. Lubberink, C.S. Levin, Studies of a next-generation silicon-photomultiplier-based time-of-flight PET/CT system, J. Nucl. Med. 58 (9) (2017) 1511–1518.
[27] I. Alberts, G. Prenosil, C. Sachpekidis, T. Weitzel, K. Shi, A. Rominger, Digital versus analogue PET in [68Ga]Ga-PSMA-11 PET/CT for recurrent prostate cancer: a matched-pair comparison, Eur. J. Nucl. Med. Mol. Imaging (2019).
[28] F. Fuentes-Ocampo, D.A. Lopez-Mora, A. Flotats, G. Paillahueque, V. Camacho, J. Duch, Digital vs. analog PET/CT: intra-subject comparison of the SUVmax in target lesions and reference regions, Eur. J. Nucl. Med. Mol. Imaging 46 (8) (2019) 1745–1750.
[29] N.C. Nguyen, J.L. Vercher-Conejero, A. Sattar, M.A. Miller, P.J. Maniawski, D. W. Jordan, Image quality and diagnostic performance of a digital PET prototype in patients with oncologic diseases: initial experience and comparison with analog PET, J. Nucl. Med. 56 (9) (2015) 1378–1385.
[30] D.A. Lopez-Mora, A. Flotats, F. Fuentes-Ocampo, V. Camacho, A. Fernandez, A. Ruiz, Comparison of image quality and lesion detection between digital and analog PET/CT, Eur. J. Nucl. Med. Mol. Imaging 46 (6) (2019) 1383–1390.
[31] C.L. Wright, K. Binzel, J. Zhang, M.V. Knopp, Advanced functional tumor imaging and precision nuclear medicine enabled by digital PET technologies, Contrast Media Mol. Imaging 2017 (2017), 5260305.
[32] I. Alberts, J.N. Hunermund, C. Sachpekidis, C. Mingels, V. Fech, K.P. Bohn, The influence of digital PET/CT on diagnostic certainty and interrater reliability in [(68)Ga]Ga-PSMA-11 PET/CT for recurrent prostate cancer, Eur. Radiol. 31 (10) (2021) 8030–8039.
[33] A. Afshar-Oromieh, E. Avtzi, F.L. Giesel, T. Holland-Letz, H.G. Linhart, M. Eder, The diagnostic value of PET/CT imaging with the (68)Ga-labelled PSMA ligand HBED-CC in the diagnosis of recurrent prostate cancer, Eur. J. Nucl. Med. Mol. Imaging 42 (2) (2015) 197–209.
[34] F. Ceci, C. Uprimny, B. Nilica, L. Geraldo, D. Kendler, A. Kroiss, (68)Ga-PSMA PET/CT for restaging recurrent prostate cancer: which factors are associated with PET/CT detection rate? Eur. J. Nucl. Med. Mol. Imaging 42 (8) (2015) 1284–1294.
[35] W.P. Fendler, J. Calais, M. Eiber, R.R. Flavell, A. Mishoe, F.Y. Feng, Assessment of 68Ga-PSMA-11 PET accuracy in localizing recurrent prostate cancer: a prospective single-arm clinical trial, JAMA Oncol. 5 (6) (2019) 856–863.
[36] S. Loeb, A. Kettermann, L. Ferrucci, P. Landis, E.J. Metter, H.B. Carter, PSA doubling time versus PSA velocity to predict high-risk prostate cancer: data from the Baltimore longitudinal study of aging, Eur. Urol. 54 (5) (2008) 1073–1080.
[37] A.V. D'Amico, M.H. Chen, K.A. Roehl, W.J. Catalona, Preoperative PSA velocity and the risk of death from prostate cancer after radical prostatectomy, N. Engl. J. Med. 351 (2) (2004) 125–135.
[38] A.V. D'Amico, A.A. Renshaw, B. Sussman, M.H. Chen, Pretreatment PSA velocity and risk of death from prostate cancer following external beam radiation therapy, JAMAJAMA 294 (4) (2005) 440–447.
[39] R. Minamimoto, I. Sonni, S. Hancock, S. Vasanawala, A. Loening, S.S. Gambhir, Prospective evaluation of (68)Ga-RM2 PET/MRI in patients with biochemical recurrence of prostate cancer and negative findings on conventional imaging, J. Nucl. Med. 59 (5) (2018) 803–808.
[40] C.O. Sahlmann, B. Meller, C. Bouter, C.O. Ritter, P. Strobel, J. Lotz, Biphasic (6)(8) Ga-PSMA-HBED-CC-PET/CT in patients with recurrent and high-risk prostate carcinoma, Eur. J. Nucl. Med. Mol. Imaging 43 (5) (2016) 898–905.
[41] S. Schmuck, M. Mamach, F. Wilke, C.A. von Klot, C. Henkenberens, J.T. Thackeray, Multiple time-point 68Ga-PSMA I&T PET/CT for characterization of primary prostate cancer: value of early dynamic and delayed imaging, Clin. Nucl. Med. 42 (6) (2017) e286-e293.
[42] L. Kabasakal, E. Demirci, M. Ocak, R. Akyel, J. Nematyazar, A. Aygun, Evaluation of PSMA PET/CT imaging using a 68Ga-HBED-CC ligand in patients with prostate cancer and the value of early pelvic imaging, Nucl. Med. Commun. 36 (6) (2015) 582–587.
[43] M. Beheshti, Z. Paymani, J. Brilhante, H. Geinitz, D. Gehring, T. Leopoldseder, Optimal time-point for (68)Ga-PSMA-11 PET/CT imaging in assessment of prostate cancer: feasibility of sterile cold-kit tracer preparation? Eur. J. Nucl. Med. Mol. Imaging 45 (7) (2018) 1188–1196.
[44] W.P. Fendler, M. Eiber, M. Beheshti, J. Bomanji, F. Ceci, S. Cho, 68Ga-PSMA PET/CT: joint EANM and SNMMI procedure guideline for prostate cancer imaging: version 1.0, Eur. J. Nuclear Med. Molecular Imaging (journal article) 44 (6) (2017) 1014–1024.